Appl. Phys. B 90, 497–502 (2008)
DOI: 10.1007/s00340-007-2827-z

Applied Physics B
Lasers and Optics

G. JIA*
H. WANG
X. LU
Z. YOU
J. LI
Z. ZHU
C. TU✉

Optical properties of Pr^{3+}-doped $SrWO_4$ crystal

Fujian Institute of Research on the Structure of Matter, Chinese Academy of Sciences, State Key Laboratory of Structural Chemistry, and National Engineering Research Center for Optoelectronic Crystalline Materials, Fuzhou, Fujian 350002, P.R. China

Received: 23 January 2007/Revised version: 31 July 2007
Published online: 13 December 2007 • © Springer-Verlag 2007

ABSTRACT The polarized absorption and emission spectra of Pr^{3+} ions in $SrWO_4$ single crystals were investigated at room temperature. The standard and modified Judd–Ofelt theories have been applied to analyze the polarized absorption spectra to determine the spectroscopic parameters, including the Judd–Ofelt intensity parameters Ω_t ($t = 2, 4, 6$), radiative transition probabilities, radiative lifetimes and branching ratios. The stimulated emission cross sections and fluorescence lifetimes of the promising laser level were obtained.

PACS 78.55.Hx; 42.70.Hj; 78.20.-e

1 Introduction

The fluorescence properties of praseodymium ions have been intensively studied in the last decades in a large variety of hosts due to their rich optical spectrum, which extends from the ultraviolet (UV) to the near infrared (NIR) [1]. Laser actions have been reported for Pr^{3+} ions in both crystals [2–5] and fibers [6]. Pr^{3+}-doped materials are also attractive in up-conversion [7], fiber amplifiers [8] and photon avalanche [9, 10].

$SrWO_4$ belongs to the scheelite family; the unit-cell parameters are $a = 5.4168$ Å, $c = 11.951$ Å, $V = 350.66$ Å^3, $Z = 4$, $D_c = 6.35$ g/cm^3 and the space group is $I4_1/a$ [11]. The crystal structure of tungstate crystals allows using these crystals as matrices for laser-active elements with nonlinear self-conversion of radiation to a new spectral range [12].

In this paper, an extensive investigation of the optical properties of Pr^{3+}-doped $SrWO_4$ crystal is described. The standard and modified Judd–Ofelt theories have been applied to analyze the absorption spectra to determine the spectroscopic parameters. We have also studied the fluorescence emission cross sections and fluorescence lifetimes of the promising laser level.

✉ Fax: +86-591-83711368, E-mail: tcy@fjirsm.ac.cn
*Present address: Department of Biology and Chemistry, City University of Hong Kong, HKSAR

2 Experimental procedure

The Pr^{3+}-doped $SrWO_4$ single crystal was grown by the Czochralski technique. The growth procedure is similar to that of Nd^{3+}:$SrWO_4$ described in our previous publication [13]. The concentration of praseodymium ions in the crystal was measured to be 0.77 wt. % by the inductively coupled plasma–atomic emission spectrometry (ICP–AES) method and the corresponding Pr^{3+} concentration is 2.09×10^{20} cm^{-3}.

The sample used for spectroscopic measurements was optically polished to flat and parallel faces. The thickness of the sample was measured to be 0.32 cm. Room temperature polarized absorption spectra of this crystal were recorded by a Perkin-Elmer UV–vis–NIR spectrometer (Lambda-900). The emission spectra of the crystal were recorded at room temperature by an Edinburgh Instruments FLS920 spectrophotometer. The fluorescence emission was analyzed with a monochromator (Acton Pro 500i) and a photomultiplier tube from Hamamatsu. The resolution of both the absorption and the fluorescence spectra is 1.0 nm.

The values of ordinary and extraordinary refractive indices of $SrWO_4$ crystal were provided in [13]. By fitting these data, Sellmeier equations of the refractive indices were obtained (λ is in unit of μm):

$$n_o^2 = 3.4383 + \frac{0.0523}{\lambda^2 + 0.001523} + 0.0049856\lambda^2; \quad (1)$$

$$n_e^2 = 3.4033 + \frac{0.0526}{\lambda^2 + 0.009456} + 0.0096059\lambda^2. \quad (2)$$

The values of the ordinary and extraordinary refractive indices are employed in the following spectroscopic calculations.

3 Results and discussion

3.1 *Absorption spectroscopy and Judd–Ofelt analysis*

The room temperature polarized absorption spectra of Pr^{3+}:$SrWO_4$ crystal are represented in Fig. 1. The terminal levels of the corresponding transitions from the $^3H_4$ ground state were assigned according to the Pr^{3+} scheme of levels in oxide hosts [14]. As can be seen from this figure, the background absorption of the Pr^{3+}:$SrWO_4$ crystal was increasing

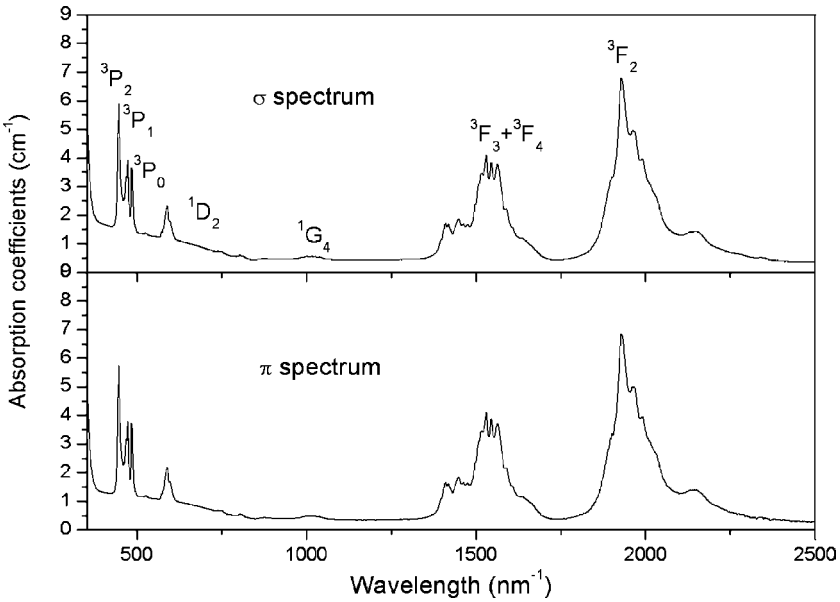

FIGURE 1 Polarized room temperature absorption spectra of Pr^{3+}:$SrWO_4$ crystal

strongly below 750 nm. In Pr^{3+}-doped $SrWO_4$ crystals, the trivalent ion (Pr^{3+}) is supposed to occupy the Sr^{2+} site and induces an excess positive charge into the crystal, which is compensated by V_{Sr} (Sr vacancies) through the formation of defect complexes $[2(Pr^{3+}_{Sr})^{\bullet} - V''_{Sr}]\,Pr^{3+}$. These defect complexes may cause an increase of the background absorption, which is comparable to those of rare earth doped $PbWO_4$ single crystals [15]. The structure of each band is due to the Stark splitting of different multiplets induced by the matrix crystal field. It is worth noting that the Pr^{3+}:$SrWO_4$ crystal shows strong absorption in the 440–500 nm range and can be effectively pumped by visible sources, such as a Xe lamp or a blue diode laser.

The Judd–Ofelt (JO) theory [16, 17] has been applied to the analysis of the absorption spectra of rare-earth ions in a variety of hosts. A brief outline of the JO theory is given in the following analysis procedure.

Considering that the interactions between magnetic dipole of Pr^{3+}-ion contributions to the absorption and emission experimental oscillator strengths are very small [18], the magnetic dipole transitions have not been taken into account in the JO calculation. The experimental line strength $S_{\mathrm{mea}}(J \to J')$ can be calculated by using the following formula [19]:

$$S_{\mathrm{mea}}(J \to J') = \frac{3ch(2J+1)}{8\pi^3 N_0 \lambda e^2} \frac{\Gamma_\pi + 2\Gamma_\sigma}{\chi_\pi + 2\chi_\sigma}\,. \tag{3}$$

Here N_0 is the Pr^{3+} concentration in the crystal, λ is the mean wavelength of the absorption band, c is the vacuum speed of light, h is Planck's constant, J is the total angular momentum of the ground state ($J = 4$ in Pr^{3+}), $\chi_{\sigma,\pi} = (n^2_{\sigma,\pi} + 2)^2/9n_{\sigma,\pi}$ is the Lorentz local field correction for the refractivity of the medium, n_σ and n_π are the values of ordinary and extraordinary refractive indices of $SrWO_4$ crystal and Γ is the integrated absorbance for each absorption band, which can be determined by

$$\Gamma = \frac{\int D(\lambda)\,\mathrm{d}\lambda}{L \log e} = \frac{2.303 \int D(\lambda)\,\mathrm{d}\lambda}{L}\,. \tag{4}$$

Here L is the sample thickness ($L = 0.32$ cm) and $D(\lambda)\,\mathrm{d}\lambda$ is the measured optical density as a function of wavelength.

According to the JO theory, the calculated line strength related to the oscillator parameters can be calculated by using the following equation:

$$S_{\mathrm{cal}}(J \to J') = \sum_{t=2,4,6} \Omega_t |\langle (S, L) J \| U^{(t)} \| (S', L') J' \rangle|^2\,. \tag{5}$$

Here Ω_t are empirically determined parameters and $\langle a \| U^{(t)} \| b \rangle$ are the doubly reduced matrix elements calculated by Carnall et al. [20]. When two absorption manifolds overlapped, the squared matrix element was taken to be the sum of the corresponding squared matrix elements.

The root-mean-square deviation of the experimental and calculated line strengths is defined by

$$\mathrm{rms}\,\Delta S = \sqrt{\sum_{i=1}^{N} (S_{\mathrm{mea}} - S_{\mathrm{cal}})^2/(N-3)}\,. \tag{6}$$

Here N is the number of absorption bands. After a least-square fitting of S_{mea} to S_{cal}, the three JO intensity parameters were obtained. The results and values of rms ΔS are presented in Table 1.

When applied to Pr^{3+}:$SrWO_4$ crystal, the standard JO theory results in large deviations between calculations and experimental data, as for other Pr^{3+}-doped materials [21, 22]. For Pr^{3+}:$SrWO_4$ crystal, the experimental and calculated line strengths of the $^3H_4 \to {}^3P_2$ transition are 1.84×10^{-20} cm^2 (σ), 1.83×10^{-20} cm^2 (π) and 0.73×10^{-20} cm^2 (σ), 0.72×10^{-20} cm^2 (π), respectively. The large deviation is usually explained by the small gap between the $4f^2$ configurations and the low-lying $4f5d$ state in Pr^{3+}, which makes the probabilities of transitions from the ground manifold to high-lying manifolds in the $4f^2$ configuration higher than those calculated by the standard JO theory [23].

To overcome this difficulty, we excluded the value of the hypersensitive transition $^3H_4 \to {}^3P_2$ in the fitting procedure,

JO parameters	The standard JO theory				The modified JO theory			
	$^3H_4 \rightarrow {}^3P_2$ with		$^3H_4 \rightarrow {}^3P_2$ without		$^3H_4 \rightarrow {}^3P_2$ with		$^3H_4 \rightarrow {}^3P_2$ without	
	σ	π	σ	π	σ	π	σ	π
Ω_2 (10^{-20} cm^2)	10.20	10.34	10.24	10.37	15.52	15.67	15.55	13.66
Ω_4 (10^{-20} cm^2)	2.08	1.96	2.12	2.0	1.78	1.66	1.80	1.73
Ω_6 (10^{-20} cm^2)	4.84	4.79	4.71	4.67	6.81	6.74	6.73	6.79
rms ΔS (10^{-20} cm^2)	0.651	0.645	0.382	0.375	0.504	0.5	0.371	0.361

TABLE 1 JO parameters and the corresponding root mean square deviations for Pr^{3+}:$SrWO_4$ crystal obtained by different methods

Excited states	$\bar{\lambda}$ (nm)	σ-polarized				π-polarized			
		$^3H_4 \rightarrow {}^3P_2$ with		$^3H_4 \rightarrow {}^3P_2$ without		$^3H_4 \rightarrow {}^3P_2$ with		$^3H_4 \rightarrow {}^3P_2$ without	
		S_{mea}	S_{cal}	S_{mea}	S_{cal}	S_{mea}	S_{cal}	S_{mea}	S_{cal}
$^3F_2$	1962	9.44	9.42	9.44	9.43	9.46	9.44	9.46	9.45
$^3F_3 + {}^3F_4$	1563	9.96	10.07	9.96	9.98	9.85	9.95	9.85	9.86
$^1G_4$	1026	0.08	0.21	0.08	0.21	0.07	0.21	0.07	0.21
$^1D_2$	591	1.00	0.43	1.00	0.42	0.98	0.42	0.98	0.42
$^3P_0$	485	0.51	0.31	0.51	0.31	0.48	0.29	0.48	0.30
$^3P_1 + {}^1I_6$	473	0.54	0.70	0.54	0.71	0.52	0.68	0.52	0.67
$^3P_2$	447	1.76	0.99	–	–	1.75	0.97	–	–

TABLE 2 Experimental and calculated line strengths of polarized absorption spectra for Pr^{3+}:$SrWO_4$ crystal obtained with the modified JO theory (S is in unit of 10^{-20} cm^2)

as is often done [2, 21]. The JO parameters have been recalculated and the results are also presented in Table 1. We can see that this method decreases the values of rms ΔS and makes minor changes in the Ω_t setting compared with that of the above standard model.

The modified JO theory as one method to improve the reliability of the JO parameters has been proposed by Dunina et al. [23]. This theory improves calculated line strengths but an additional parameter has to be introduced. The modified line-strength formula is expressed as

$$S_{cal} = S_{cal}(\text{standard})\left[1 + \frac{E_i - 2E_f^0}{E_{5d} - E_f^0}\right]. \quad (7)$$

Here the standard line strength is from (6), E_i is the energy of the final state, E_{5d} is the energy of the lowest $4f5d$ state and E_f^0 is the average energy over the $4f^2$ states. The values of E_f^0 and E_{5d} are 10 000 cm^{-1} and 60 000 cm^{-1}, respectively [24]. On the basis of the modified JO theory, both calculations with and without the $^3H_4 \rightarrow {}^3P_2$ transition were obtained. All the results are given in Table 1 for comparison. From the table, we can see that the modified JO theory without considering the $^3H_4 \rightarrow {}^3P_2$ transition gives the best fitting results for our experimental and calculated line strengths. Table 2 shows the experimental and calculated line strengths for Pr^{3+}:$SrWO_4$ crystal obtained with either case of the modified JO theory.

In the following analysis, the JO parameters determined by the modified JO theory without the $^3H_4 \rightarrow {}^3P_2$ transition are adopted. In the anisotropic crystal, the relations between the effective JO parameters Ω_t^{eff} and the polarized JO parameters $\Omega_{t,\sigma(\pi)}$ ($t = 2, 4, 6$) should be $\Omega_t^{\text{eff}} = (2\Omega_{t,\sigma} + \Omega_{t,\pi})/3$ [25]. So, the effective JO parameters of Pr^{3+}:$SrWO_4$ crystal are $\Omega_2^{\text{eff}} = 14.9 \times 10^{-20}$ cm^2, $\Omega_4^{\text{eff}} = 1.8 \times 10^{-20}$ cm^2 and $\Omega_6^{\text{eff}} = 6.8 \times 10^{-20}$ cm^2. Table 3 gives the JO parameters for Pr^{3+} doped in other hosts.

Using the obtained emission line strengths, the radiative transition probabilities $A(J \rightarrow J')$ can be determined by the following expressions:

$$A(J \rightarrow J') = \frac{64\pi^4 e^2}{3h(2J+1)\bar{\lambda}^3}\frac{n(n^2+2)^2}{9} \times \sum_{t=2,4,6} \Omega_t |\langle (S, L)J \| U^{(t)} \| (S', L')J' \rangle|^2 \times \left[1 + \frac{E_i - 2E_f^0}{E_{5d} - E_f^0}\right], \quad (8)$$

$$A_T(J) = \sum_{J'} A(J \rightarrow J'). \quad (9)$$

Using the reduced matrix elements for Pr^{3+} ions presented previously [28], the radiative transition probabilities are obtained. Then, using the radiative lifetime $\tau_r = 1/A_T(J)$, the mathematical formula for the fluorescent branching ratio was found by [29]

$$\beta(J') = \frac{A(J \rightarrow J')}{A_T(J)}. \quad (10)$$

The calculated radiative transition probabilities, the branching ratios and the radiative lifetimes for different transition levels are presented in Table 4.

Material	Ω_2 (10^{-20} cm^2)	Ω_4 (10^{-20} cm^2)	Ω_6 (10^{-20} cm^2)	Ref.
$NaBi(MoO_4)_2$	9.8	12.8	1.3	[18]
$KGd(WO_4)_2$	19.50	7.31	4.86	[26]
$PbWO_4$	19.76	5.57	7.30	[27]
$SrWO_4$	14.9	1.8	6.8	This work

TABLE 3 The JO intensity parameters of Pr^{3+}-doped crystals

Transition	Wavelength (nm)	A (s^{-1})	β	τ_r (μs)
$^3P_0 \rightarrow {}^1D_2$	2584	56	0.0005	9.5
$^1G_4$	924	461	0.004	
$^3F_4$	728	2690	0.03	
$^3F_3$	697	0	0	
$^3F_2$	643	79290	0.75	
$^3H_6$	617	10030	0.10	
$^3H_5$	538	0	0	
$^3H_4$	488	13010	0.12	
$^1D_2 \rightarrow {}^1G_4$	1439	2070	0.17	80.9
$^3F_4$	1013	7180	0.58	
$^3F_3$	971	501	0.04	
$^3F_2$	855	523	0.04	
$^3H_6$	810	280	0.02	
$^3H_5$	689	16	0.001	
$^3H_4$	594	1798	0.15	

TABLE 4 Calculated radiative transition probabilities, branching ratios and radiative lifetimes for different transition levels of Pr^{3+}:$SrWO_4$ crystal

3.2 *Fluorescence spectroscopy and stimulated emission cross sections*

The room temperature polarized emission spectra of Pr^{3+}:$SrWO_4$ excited by 447-nm pumping are shown in Fig. 2. The fluorescence of Pr^{3+}:$SrWO_4$ crystal in the visible region mainly consists of emissions from the metastable ^3P_j $(j = 0, 1, 2)$ manifolds. The most intensive emission around 645 nm was detected and assigned to the transition $^3P_0 \rightarrow {}^3F_2$.

The room temperature polarized fluorescence spectra in the spectral region 800–1300 nm of this crystal excited by 447-nm pumping are shown in Fig. 3. The fluorescence spectra in the infrared region were mainly assigned to the transitions from the $^1D_2$ manifold. There are two main emission bands located around 866 nm and 1043 nm, corresponding to $^1D_2 \rightarrow {}^3F_2$ and $^1D_2 \rightarrow {}^3F_4$ transitions, respectively.

The emission cross section is an important parameter influencing the potential laser performance. The stimulated emission cross section can be estimated from the room temperature fluorescence spectra by using the Füchtbauer–Ladenburg (F–L) formula [30]

$$\sigma_{em}(\lambda) = \frac{\lambda^5 \beta}{8\pi c n^2 \tau_r} \frac{3I_{\sigma,\pi}(\lambda)}{\int [2I_\sigma(\lambda) + I_\pi(\lambda)]\lambda \, d\lambda} . \quad (11)$$

Here $I_{\sigma,\pi}(\lambda)$ is the experimental emission intensity for the σ- or π-polarization spectrum. With the present data, we can estimate the emission cross sections of the $^3P_0 \rightarrow {}^3F_2$ transition and transitions from the $^1D_2$ manifold. Table 5 shows the peak emission wavelengths and cross sections of several main transitions for Pr^{3+}:$SrWO_4$ crystal. It is worth noting that the peak emission cross sections of the $^3P_0 \rightarrow {}^3F_2$ red laser channel are 1.9×10^{-18} cm^2 (σ) and 1.7×10^{-18} cm^2 (π). The values are larger than those of Pr^{3+}-doped $LiYF_4$ crystal (0.3×10^{-19} cm^2 for the π-polarization and 2.1×10^{-19} cm^2 for the σ-polarization), in which a red laser has been realized [4, 31].

3.3 *Fluorescence lifetime*

Figure 4 shows the luminescence decay curve of the $^3P_0 \rightarrow {}^3H_4$ transition at the wavelength of 490 nm excited by 447-nm pumping. It was found that the decay does not fit a single exponential, but could be described by a double exponential. The lifetimes of τ_1 and τ_2 components are estimated to be 4.3 and 0.98 μs, respectively.

So, the mean value of the lifetime can be obtained by using the following equation:

$$\tau_m = \int_0^\infty I(t) \, dt , \quad (12)$$

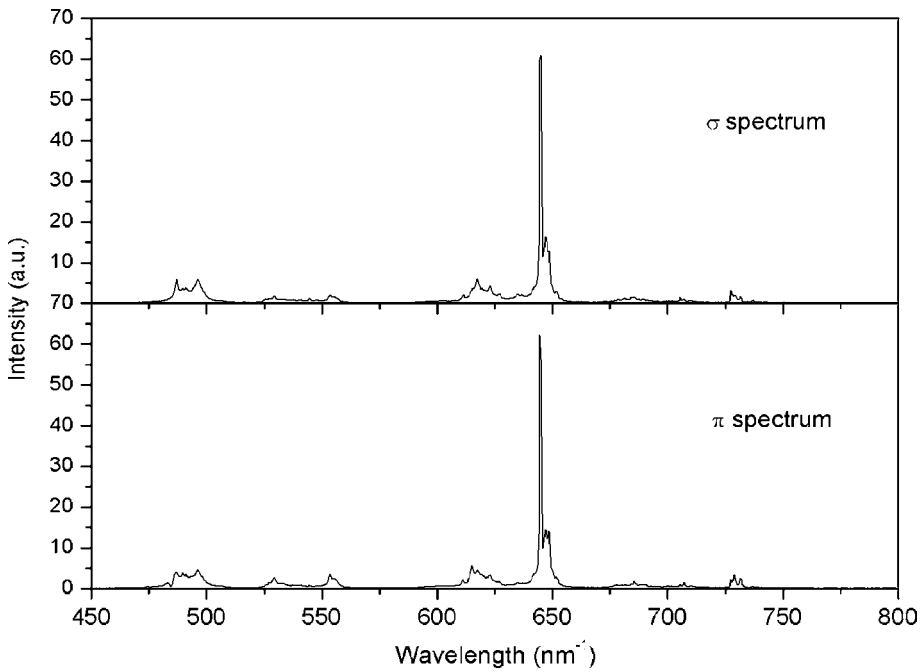

FIGURE 2 Visible polarized room temperature fluorescence spectra of Pr^{3+}:$SrWO_4$ crystal excited by 447-nm pumping

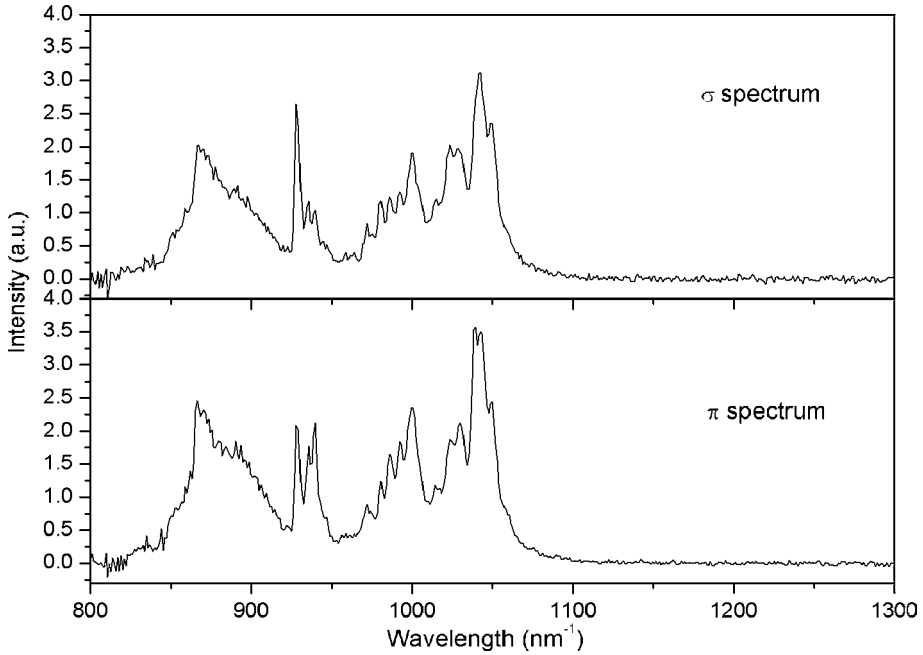

FIGURE 3 Infrared polarized room temperature fluorescence spectra of Pr^{3+}:$SrWO_4$ crystal excited by 594-nm pumping

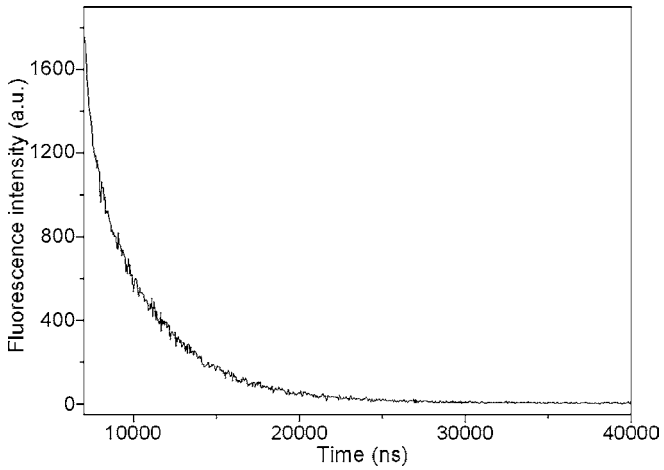

FIGURE 4 Room temperature luminescence decay curve at 490 nm excited by 447-nm pumping

Transition	Wavelength (nm)	σ_σ (10^{-20} cm^2)	σ_π (10^{-20} cm^2)
$^3P_0 \rightarrow {}^3H_4$	489	1.5	1.5
$^3P_0 \rightarrow {}^3H_6$	617	6.3	4.5
$^3P_0 \rightarrow {}^3F_2$	645	187	173
$^3P_0 \rightarrow {}^3F_4$	732	5.3	3.6
$^1D_2 \rightarrow {}^3F_2$	866	0.2	0.3
$^1D_2 \rightarrow {}^3F_4$	1043	6.6	7.4

TABLE 5 The stimulated emission cross sections of main transitions for Pr^{3+}:$SrWO_4$ crystal

where $I(t)$ represents the normalized decay curve. From the calculation, the mean value of the fluorescence lifetime was 5.0 μs. The luminescent quantum efficiency $\eta = \tau_m/\tau_r$ is 52.6% for the $^3P_0$ level. It shows that Pr^{3+}:$SrWO_4$ crystal has high luminescent quantum efficiency.

The mean fluorescence lifetime τ_m is a more reliable parameter, especially for the estimation of the laser threshold and efficiency [32]. Even the fluorescence lifetime of the $^3P_0$ level for the Pr^{3+}:$SrWO_4$ crystal is relatively short. The values of the emission cross section σ_q^{em} and the mean fluorescence lifetime τ_m for the $^3P_0 \rightarrow {}^3F_2$ transition (9.50×10^{-18} cm^2 μs (σ-polarization) and 8.50×10^{-18} cm^2 μs (π-polarization) are larger than those of other tungstate crystals, such as 2.86×10^{-18} cm^2 μs (π-polarization) of the Pr^{3+}:$PbWO_4$ crystal [33] and 1.70×10^{-18} cm^2 μs ($E//X$) of the Pr^{3+}:$La_2(WO_4)_3$ crystal [27, 32]. Therefore, the $^3P_0$ level of Pr^{3+}:$SrWO_4$ crystal is a promising luminescent laser level.

4 Conclusion

The main spectroscopic properties of Pr^{3+} ions in $SrWO_4$ single crystals have been determined for the σ- and π-polarizations. The polarized absorption spectra were analyzed by the standard and modified JO theories, and the best fitting results were obtained by the modified JO theory without the $^3H_4 \rightarrow {}^3P_2$ transition. The stimulated emission cross sections of some typical fluorescence transitions were estimated. The fluorescence lifetime of the $^3P_0$ level was determined. Results of this work demonstrate that $SrWO_4$ crystal doped with Pr^{3+} ions has good spectroscopic properties and may be a potential candidate for solid-state laser materials.

ACKNOWLEDGEMENTS This work was supported by the Natural Science Foundation of Fujian Province of China (E0410028), the Frontier & Interdisciplinary Project of Fujian Institute of Research on the Structure of Matter, CAS and the Innovative Project of the Chinese Academy of Sciences (KJCX2-SW-h05 and CXJJ-182).

REFERENCES

1 S. Kück, I. Sokólska, M. Henke, T. Scheffler, E. Osiac, Phys. Rev. B **71**, 165 112 (2005)
2 J.M. Sutherland, P.M.W. French, J.R. Taylor, Opt. Lett. **21**, 797 (1996)
3 L.D. Merkle, B. Zandi, R. Moncorgé, Y. Guyot, H.R. Verdun, B. McIntosh, J. Appl. Phys. **79**, 1849 (1996)
4 T. Sandrock, T. Danger, E. Heumann, G. Huber, B.H.T. Chai, Appl. Phys. B **58**, 149 (1994)

5 R.G. Smart, D.C. Hanna, A.C. Tropper, S.T. Davey, S.F. Carter, D. Szebesta, Electron. Lett. **127**, 1307 (1991)
6 A. Richter, Electron. Lett. **41**, 794 (2005)
7 E. Osiac, E. Heumann, G. Hubert, S. Kuck, E. Sani, A. Toncelli, M. Tonelli, Appl. Phys. Lett. **82**, 3832 (2003)
8 R.C. Schimmel, A.J. Faber, H. de Waardt, R.G.C. Beerkens, G.D. Khoe, J. Non-Cryst. Solids **284**, 188 (2001)
9 J.S. Chivian, W.E. Case, D.D. Eden, Appl. Phys. Lett. **35**, 124 (1979)
10 D.B. Gatch, W.M. Dennis, W.M. Yen, Phys. Rev. B **62**, 10790 (2000)
11 E. Gurmen, E. Daniels, J.S. King, J. Chem. Phys. **5**, 1093 (1971)
12 L.I. Ivleva, T.T. Basiev, I.S. Boronina, P.G. Zverev, V.V. Osiko, N.M. Polozkov, Opt. Mater. **23**, 439 (2003)
13 G. Jia, C. Tu, A. Brenier, Z. You, J. Li, Z. Zhu, Y. Wang, B. Wu, Appl. Phys. B **81**, 627 (2005)
14 A.A. Kaminskii, H.J. Eichler, Phys. Stat. Solidi B **185**, K85 (1994)
15 Y.L. Huang, X.Q. Feng, Z.H. Xu, G.J. Zhao, G.S. Huang, S.G. Li, Solid State Commun. **127**, 1 (2003)
16 B.R. Judd, Phys. Rev. **127**, 750 (1963)
17 G.S. Ofelt, J. Chem. Phys. **37**, 511 (1962)
18 A. Mendez-Blas, M. Rico, V. Volkov, C. Cascales, C. Zaldo, C. Coya, A. Kling, L.C. Alves, J. Phys.: Condens. Matter **16**, 2139 (2004)
19 D. Jaque, O. Enguita, U. Caldino, M.O. Ramirez, J. Garcia Sole, J. Appl. Phys. **90**, 561 (2001)
20 W.T. Carnall, P.R. Fields, K. Rajnak, J. Chem. Phys. **49**, 4429 (1968)
21 A. Brenier, I.V. Kityk, J. Appl. Phys. **91**, 232 (2001)
22 B. Savoini, J.E. Muñoz Santiuste, R. González, Phys. Rev. B **56**, 5856 (1997)
23 E.B. Dunina, A.A. Kaminskii, A.A. Kornienko, K. Kurbanov, K.K. Pukhov, Sov. Phys. Solid State **32**, 290 (1990)
24 P. Goldner, F. Auzel, J. Appl. Phys. **79**, 7972 (1996)
25 Y.J. Chen, X.Q. Lin, Z.D. Luo, Y.D. Huang, Chem. Phys. Lett. **397**, 282 (2004)
26 C. Zaldo, M. Rico, C. Cascales, M.C. Pujol, J. Massons, M. Aguiló, F. Díaz, P. Porcher, J. Phys.: Condens. Matter **12**, 8531 (2000)
27 F.B. Xiong, Z.D. Luo, Y.D. Huang, Appl. Phys. B **80**, 321 (2004)
28 D.K. Sardar, C.C. Russell III, J. Appl. Phys. **95**, 5334 (1996)
29 W.F. Krupke, IEEE J. Quantum Electron. **QE-10**, 450 (1974)
30 B.M. Walsh, N.P. Barnes, B. Di Bartolo, J. Appl. Phys. **83**, 2772 (1998)
31 D.S. Knowles, Z. Zhang, D. Gabbe, H.P. Jenssen, IEEE J. Quantum Electron. **QE-24**, 1118 (1988)
32 G.B. Loutts, C. Bonner, C. Meegoda, H. Ries, M.A. Noginov, N. Noginova, M. Curley, P. Venkateswarlu, A. Rapaport, M. Bass, Appl. Phys. Lett. **71**, 303 (1997)
33 F.B. Xiong, X.H. Gong, Y.F. Lin, Y.J. Chen, Q.G. Tan, Z.D. Luo, Y.D. Huang, Appl. Phys. B **86**, 279 (2007)